Report for 2005FL101B: Mechanisms and Modeling of Soft-Bed Nutrient Release in Lakes

Publications

- Conference Proceedings:
  - Jain, M., Mehta, A. J., Hayter, E. J., and Di, J., 2006. Fine sediment resuspension and nutrient transport in Newnans Lake, Florida, submitted for publication in the proceedings of INTERCOH 2005 meeting, T. Kusuda, H. Yamanishi and E. Toorman eds., Elsevier, Amsterdam.

Report Follows

Fine Sediment Resuspension and Nutrient Transport in Newnans Lake, Florida

Mamta Jain[1], Ashish J. Mehta[1], Earl J. Hayter[2] and Jian Di[3]

[1] Department of Civil and Coastal Engineering
University of Florida, Gainesville, FL 32611, U.S.A.

[2] U.S. Environmental Protection Agency
Athens, GA 30605, U.S.A.

[3] Environmental Sciences Division
St. Johns River Water Management District
Palatka, FL 32178, U.S.A.

Abstract

The character of fine sediment resuspension and nutrient transport were examined for Newnans Lake in north-central Florida. Physical and water quality parameters were monitored over a period of eight months in the lake and also in the inflow and outflow streams. From the hydraulic point of view, this lake may be thought of as a shallow and wide open channel in which inflowing sediment transport is modulated by wind effects. Suspended sediment concentration (SSC) response to wind speed was found to occur over a wide frequency band, with spectral peaks that seemingly correlate with lunar motion. On a time-mean basis, wind kinetic energy maintains the particulate matter as a Benthic Suspended Sediment Layer with a mean height of about 0.80 m and SSC of about 70 mg L^{-1}. The suspended sediment mass per unit bed area is equivalent to less than 1 mm thick bed layer, indicating that there is little interaction between the ~ 2 m thick muck in the lake and the water column. Nutrient mass balance analysis is simplified because dissolved nutrient loads are close or nearly equal to total loads, with minor to negligible contributions from the low-concentration particulate matter. Mass balances for

phosphorus and nitrogen indicate periods of days over which the lake acts both as a net exporter and a net importer of these nutrients.

INTRODUCTION

In recent decades several lakes in Florida have attained high trophic levels and their water quality has become a matter of concern to the management agencies. Such lakes tend to be laden with fine-grained, organic-rich muck at the bottom, which can be a repository as well as a source of phosphorus and nitrogen necessary for the eutrophication. Since these nutrients are typically derived from inflow streams, an important question bearing on water quality management is the role of these streams and sediment resuspension in the lake in governing nutrient loads in the outflow streams. In lakes where water throughput is steady and sufficiently high to ensure low residence times for water parcels and suspended matter, an assessment of water quality does not always require a lengthy diagnostic treatment. On the other hand, where throughput is high only on an episodic basis, the transport process can be complex because under normal conditions effects due to stream discharge and wind tend to occur at uncorrelated frequencies. Given that most lakes in Florida experience episodic forcing, as a paradigm we examined Newnans Lake in north-central Florida, with the aim to assess its sediment and nutrient transport regimes. A factor as well in the selection of this lake was the State of Florida's plan to restore the lake's water quality in the coming years.

Although water quality and biological assays have been carried out in the lake, prior information on sediment and nutrient transport in the combined lake-and-stream system is sparse. Therefore, in 2004 we conducted a field campaign to obtain time-series and discrete sampling measurements related to factors characterizing the transport regime.

Data included stream discharges, wind-induced hydrodynamic parameters, suspended solids concentration (SSC) and concentrations of chemical species related to the nutrients (phosphorus and nitrogen). Observations based on these data are summarized, and an effort has been made to characterize the sediment and nutrient transport regimes.

SITE AND METHOD OF ANALYSIS

The 7 km long and 4 km wide lake in north-central Florida (Fig. 1) has a surface area of about 27 km^2. The lake has up to 2 meters of muck, and portions of the littoral zone are densely covered by floating macrophytes that have contributed to the organic component of the muck. The maximum depth of water is about 3.9 m in the middle of the lake and the mean depth about 1.6 m. Thus the volume of muck, about $2x10^7$ m^3, constitutes over one-half the lake volume above the sandy substrate beneath the muck. The muck is watery with a mean dry density of about 100 kg m^{-3}, which corresponds to a solid mass of two million metric tons. At the present rate of sediment inflow, this amount would be equivalent to over eight centuries of sediment from the drainage basin.

The lake drainage area covers approximately 300 km^2 and supplies the majority of the runoff through two main tributaries, Hatchet Creek and Little Hatchet Creek, both at the northern end of the lake. A smaller stream called Bee Tree Creek confluences with Hatchet Creek north of its outlet at the lake. Overflow drains out of Prairie Creek at the southern end and empties into a large basin called Paynes Prairie. The majority of the lake shoreline is surrounded by a canopy of local forest trees.

At the site shown in Fig. 1, a three-legged aluminum-frame platform schematically drawn in Fig. 2 was installed in December 2003, and fully operated from early January to early September in 2004. Transducers (Table 1) were deployed for measuring wind

velocity, air and water temperatures, total water pressure and pore water pressure within muck, horizontal and vertical current velocity components, wave-induced acceleration in muck, SSC in water (at three levels) and water samples (two levels).

Data on current velocity, total water pressure, pore water pressure, and fluid (muck) acceleration were collected in the digital mode. Sampling was on the hour for 5 minutes at a bursting frequency of 10 Hz. Wind speed, air temperature, water temperature, air pressure and SSC data collection was in the analog mode with 2-min mean values recorded every one-half hour. All data were telemetered on real-time basis via a modem and cell-phone connection to the University of Florida for storage and analysis.

At stations BTC, HC, LHC and PC, daily discharges were measured by the St. Johns River Water Management District (SJRWMD). Also measured at these stations and at HCW were water quality parameters. At NL daily lake water level data were recorded, and at GNV (Gainesville Regional Airport) daily values of atmospheric parameters were recorded by the airport authority (Jain et al., 2005). A description of the bottom sediment characteristics has been presented by Gowland et al. (2005). For the 0.4 m thick top layer of bottom sediment relevant to the present study the ranges of bed parameters were as follows: Stokes' settling diameter of aggregated particles 26 to 38 μm, organic matter 43 to 52% by weight, wet bulk density 1,020 to 1,050 kg m^{-3}, and particle density 1,600 to 2,100 kg m^{-3}.

The vertical profile of the bed bulk density obtained by a 76 mm diameter PVC push-core is shown in Fig. 3. As indicated, the accelerometer and the pore pressure gauge were both located 0.2 m below the muck surface. This was arranged in order to determine if the muck heaved due to wind wave action. At that depth the (wet bulk) density was

approximately 1,046 kg m^{-3}, which indicated that the muck had negligible (bulk) shear strength (Mehta, 1991).

The erodibility characteristics of the bottom muck were determined in laboratory tests reported by Gowland et al. (2005). Bed erosion was modeled by the equation

$$\varepsilon_e = \varepsilon_N (\tau_{cw} - \tau_s) \tag{1}$$

where ε_e is the erosion flux, ε_N is the erosion flux constant, τ_{cw} is the peak value (over the wave period) of the combined bed shear stress due to current and waves, and τ_s is the bed shear strength against erosion. For modeling sediment transport, a lake-mean value of ε_N = 1.0 kg m^{-2} s^{-1} Pa^{-1} was selected, and τ_s was determined by calibration against measured SSC time-series. We used the following functions to describe the settling flux ε_s:

$$\varepsilon_s = w_o C, \quad C < C_o; \qquad \varepsilon_s = \frac{a C^n}{\left(b^2 + C^2\right)^m}, \quad C \geq C_o \tag{2}$$

in which C denotes SSC and C_o (= 0.1 kg m^{-3}) is the concentration limit below which w_s tends to be practically free of the effect of inter-particle collisions and is assumed constant (w_0 = 1.15x10^{-4} m s^{-1}). The coefficients *a, b, n,* and *m* were taken as 0.17, 2.4, 1.8 and 1.8, respectively.

The shear stress τ_{cw} was determined from the method of Soulsby et al. (1993). To being with, the current-induced shear stress τ_c was determined from

$$\tau_c = \left[\frac{0.4}{\ln(0.033h/k_s) - 1}\right]^2 \rho_w u_m^2 \tag{3}$$

where h is the water depth, k_s is the Nikuradse bed roughness, ρ_w is the fluid (water) density and u_m is the near-bottom current velocity. The wave-induced bed shear stress was calculated from

$$\tau_w = 0.5 f_w \rho_w \left(\frac{H\sigma}{2\sinh kh} \right)^2 \tag{4}$$

where f_w is the wave friction factor, H is the wave height, $\sigma = 2\pi / T$ is the wave angular frequency, $k = 2\pi / L$ is the wave number, T is the wave period and L is the wavelength. The wave friction factor was obtained from

$$f_w = 0.3, \quad \frac{a_b}{k_s} \le 1.57; \quad f_w = 0.00251 \exp\left[5.21 \left(\frac{a_b}{k_s} \right)^{-0.19} \right]; \quad \frac{a_b}{k_s} > 1.57 \tag{5a}$$

where the wave-induced bottom excursion amplitude a_b is given by the Airy linear wave theory (Dean and Dalrymple, 1991) as

$$a_b = \frac{H}{2\sinh kh} \tag{5b}$$

The current and wave shear stresses are superimposed using

$$\begin{aligned} Y &= 1 + a_o X^M (1 - X)^N \\ Y &= \frac{\tau_{cw}}{\tau_c + \tau_w} \\ X &= \frac{\tau_c}{\tau_c + \tau_w} \end{aligned} \tag{6a}$$

where

$$a_o = \left(a_1 + a_2 \left| \cos\varphi \right|^I \right) + \left(a_3 + a_4 \left| \cos\varphi \right|^I \right) \log \left\{ \frac{f_w}{\left[0.4 / \left\{ \ln(0.033 h / k_s) - 1 \right\} \right]^2} \right\} \tag{6b}$$

with analogous expressions for M and N. The quantity φ is the angle between the current stress vector and the wave stress vector. The coefficients a_i, M_i, N_i (i = 1 to 4) and I are given in Table 2, as prescribed by Soulsby et al. (1993).

The above formulation for calculating τ_{cw} requires values of h, H, T, L, u_m, φ and k_s. For the water depth h a recent bathymetric survey was used (Jain et al., 2005). The wave

length L is dependent on height H and period T, and the Airy theory was used to relate the three, with H and T obtained from measurements.

For determining u_m and k_s we used the public domain numerical model Environmental Fluid Dynamics Code (EFDC), a three-dimensional, hydrostatic flow model with a compatible sub-model for sediment transport. The Cartesian coordinate system was used in the horizontal plane, and the vertical coordinate was stretched to follow the bottom contours and the free surface. In the model the finite difference method is used to solve the governing equations, and an external/internal mode splitting procedure is used to increase numerical efficiency (Hamrick, 1992; 1996; 2000; Park et al., 2001). As the model generated the instantaneous current velocity vectors throughout the lake and the wind direction was known in principle, the angle φ could have been determined. However, for simplicity of treatment, φ was set equal zero everywhere.

The sediment sub-model of EFDC solves the mass balance equation for SSC. Due to a small numerical diffusion inherent in the scheme used to solve this equation, the horizontal diffusion terms are omitted. Equations (1) and (2) were used to calculate the erosion and deposition fluxes required as the important bottom boundary conditions for the sub-model.

OBSERVATIONS

Monthly values of the physical parameters listed in Tables 3 and 4 characterize the lake as one subject to moderate climatic changes. The directionally variable winds (Fig. 4) are low-energy; the mean wind speed rarely exceeds 10 m s^{-1}. High speeds in June-September were due to the passage of Hurricanes Frances and Jeanne over northern

Florida in September. Current speed measured at the platform was on the order of only a few millimeters per second (Table 5).

Although the monthly maximum value of the significant wave height (derived from water pressure data) was 0.28 m in June, typical values ranged between 0.14 and 0.16 m. The maximum value of the modal period was 1.4 s. Besides low wind speeds, wave action in the lake is limited by shallow water depths and short wind fetches. The maximum fetch at the platform was less than 4 km.

It proved to be difficult to determine the precise depth of the muck surface at the platform because SSC changed gradually with depth, so the bed was not defined by a distinct interface. The effective water depth was therefore estimated by comparing the measured amplitudes of wave orbital current and vertical acceleration (Table 4) with the same quantities calculated from the Airy theory in which the water depth was adjusted until a match occurred. This led to a value of depth $h = 2.1$ m.

In Table 3, discharge out of Prairie Creek does not correlate with rainfall because of the significant effect of evapotranspiration on the lake's water budget, especially during the summer months (May-August). In contrast, contribution from groundwater or seepage is believed to be minor. Due to shallow water, significant thermoclines typically do not develop even as pycnoclines due to SSC and nutrients persist. Vertical gradients in SSC are evident from the values given in Table 5.

The main tributary to the lake is Hatchet Creek, as Little Hatchet Creek contributes, on the average, only about 20% of the total inflow. However, under normal conditions neither discharge from Hatchet Creek nor wind is dominant as a transporting agent in the lake proper. As a result, the combined influence of discharge and wind on SSC is

manifested as a noisy signal spread over a wide frequency band. This is evident in Fig. 5, in which a sample of the measured SSC time-series (by OBS-2) suggests multi-frequency response. The running average curve represents frontal oscillations on the order of days, and these fluctuations are modulated by higher frequency diurnal contributions.

Figure 6 shows wind, air temperature and SSC spectra derived from a 90-day long (January-March) time-series. Three noteworthy peaks are seen, and they seem to be related to lunar tidal harmonics. These are the lunar quarter-phase period of 6.8 solar days, its second harmonic of 3.4 d and the lunar diurnal period of 1.08 d. A fourth peak corresponding to about 0.5 d could be the luni-solar semi-diurnal period (11.97 hr). Sea breeze is known to respond to tidal effects (Richards, 2003), and is the seeming explanation for the coincidence of the frequencies with lunar motion. Nonetheless, the occurrence of this effect is somewhat surprising because the lake is approximately 100 km from the Atlantic coast, a substantial distance. A further study of meteorological forcing is essential before a definitive conclusion can be reached as to the interpretation of the observed spectral peaks.

From Tables 3 and 4 we observe that monthly mean wind speeds range between 2.5 and 4.1 m s^{-1}, and monthly peak winds between 8.9 and 12.6 m s^{-1}. The generally low mean and peak speeds point to a practically "eventless" period of eight months. Similarly, the Prairie Creek discharge range of 0.21 to 1.24 m^3 s^{-1} indicates consistently low throughput over the same period. Higher wind speeds in September accompanying the hurricanes also brought higher rainfall and creek discharges. On September 9, following the nearest passage of Frances on September 4, discharge in Prairie Creek rose to 22 m^3 s^{-1}. Then, on September 30, following Jeanne on September 25, the discharge

further increased to 27 m^3 s^{-1}. 2-min mean gusts attained maximum values of 20 m s^{-1} during Frances and 15 m s^{-1} during Jeanne. It should be pointed out, however, that in the recent past hurricanes have seldom led to high discharges coupled with high winds in this region of Florida. More common occurrences are those of high discharge without high wind, as during the El Niño event of February 1998 when the peak discharge in Prairie Creek was 17 m^3 s^{-1}.

Wave related parameters showed a weak but identifiable dependence on wind speed. A typical set of data is from the month of February. In Fig. 7 the significant wave height is seen to increase with wind speed at a nearly linear rate. The cutoff line at 2 m s^{-1} corresponds to the limit of sensitivity of the wave pressure gage. In Fig. 8 the wave modal period is also seen to increase with wind speed, albeit in a non-linear way. In Fig. 9, plots of the horizontal and vertical wave velocity amplitudes are given. These amplitudes are consistent with the wave height (Fig. 7) and period (Fig. 8) data.

To help interpret the relationship between SSC (C) and wind speed (U), each was represented by the sum of a low-frequency component (marked by an overbar) associated with frontal wind events and a higher frequency component (with a hat) associated with daily (diurnal) events:

$$U = \bar{U} + \hat{U} \; ; \qquad C = \bar{C} + \hat{C} \tag{7}$$

In Figs. 10a,b data from OBS-2 have been plotted. The $\bar{C}$ values show a weak yet recognizable linear dependence on $\bar{U}$ ($\bar{C} = \bar{a}\bar{U} + \bar{b}$). In Fig. 10b, $\hat{C}$ shows little dependence on $\hat{U}$. Nevertheless, for the convenience of data interpretation, one may postulate the occurrence of a linear relationship of the form $\hat{C} = \hat{a}\hat{U}$. Values included correspond to times when $\hat{U}$ and $\hat{C}$ were increasing together, i.e., when both quantities

had positive slopes. Data at times when either (or both) slope of a $\hat{U}, \hat{C}$ pair was negative had to be discarded in order to avoid even more excessive data scatter than observed. A likely reason for this lack of response of $\hat{C}$ to $\hat{U}$ may be that the ratio of the wave period (~ 1 s) to the sediment settling time lag (~10^{-4} m s^{-1}) was on the order of 10^{-4}, a very small value. As a result, and coupled with a directionally variable wind-wave field which complicated the role of waves, discrete oscillations in SSC induced by settling and entrainment could not be clearly gleaned from the data.

Taking $\bar{U}$ = 4 m s^{-1} and $\hat{U}$ = 0.5 m s^{-1} as representative values we obtain $\hat{C}/\bar{C}$ = 0.4/16.5 = 0.02. In Table 6 this ratio is calculated for the three OBSs. Also given are the coefficients $\bar{a}, \bar{b}$ and $\hat{a}$. To enhance the generality of the observations, results are included from February (representing the winter climate) as well as May (representing summer), when unfortunately only two of the three sensors were operating. Overall, the $\hat{C}/\bar{C}$ ratio ranges from 0.02 to 0.11, indicating that diurnal variations modulate the frontal amplitudes by a factor of 2% to 11%. In other words, daily winds seem to play a lesser role compared to "weekly" wind events in resuspending sediment.

In Fig. 11, the suspended sediment load S is plotted against discharge Q for Prairie Creek. The mean trend is seen to be linear, which implies a constant SSC (C = 16 mg L^{-1}), because by definition $S = CQ$. These data are based on samples collected at mid-depth in the creek, and in terms of elevation they are compatible with data recorded by OBS-2 in the lake. Data from Hatchet and Little Hatchet Creek also indicated similar trends, with mean concentrations given below.

Hatchet (+ Bee Tree) Creek	8 mg L^{-1}
Little Hatchet Creek	11 mg L^{-1}
Prairie Creek	16 mg L^{-1}

Constant SSC in the creeks implies that sediment transport in these streams is supply-limited. The inflow creek beds appear to consist of sediment that does not erode even at high discharges, a characteristic of channels in clear-water equilibrium. In Prairie Creek, SSC is limited by supply from the lake.

FLOW FIELD AND SEDIMENT TRANSPORT

For simulation of the flow field and sediment transport using the EFDC model, the Cartesian grid for the lake was composed of 1078 computational cells. The horizontal dimension of each cell was 150 m (N-S) by 100 m (E-W). Three stretched horizontal layers were used to represent the water column. At the lake boundary cells representing the three creeks, measured discharge time-series were supplied. Also inputted into the model were time-series of wind, precipitation and evapotranspiration. The wave height and period fields required for bed shear stress calculation were estimated from relationships with wind speed of the type shown in Figs. 7 and 8, respectively. At the cell containing the water level gauge (NL in Fig. 1), the measured time-series was compared with simulation. The hot-start calibration period was from day 5 to 54, and the best agreement was obtained using a bed roughness parameter k_s = 0.01 m. Validation covered the period from day 60 to 110.

A comparison between measured and simulated water levels in the lake in Fig. 12 during validation shows a reasonable agreement, with a maximum difference of about 0.08 m before day 99 and about -0.02 m afterwards. During the 50-day period the simulated water volume out of Prairie Creek was 7.62×10^6 m^3, which differed from the measured value (7.73×10^6 m^3) by less than 2%.

Figure 13 shows the simulated surface velocity vectors in the lake for a selected southwesterly wind of 7 m s^{-1} and a steady outflow of 1.3 m^3 s^{-1} out of Prairie Creek in February 2004. Due to the throughput from the inflow creeks towards Prairie Creek, the vectors point southward, with the exception of littoral circulation gyres generated by local boundary geometry. The velocities were everywhere below 0.03 m s^{-1}. It is also noteworthy that in the southern part of the lake the flow is channelized through a seemingly narrow neck. A similar simulation without wind produced lower velocities, which fell by about 40% in the neck area.

The fine sediment transport sub-model in EFDC was calibrated by adjusting the erosion shear strength τ_s (= 0.035 Pa) to achieve agreement between measured and simulated time-mean SSC values at the platform. Figure 14 shows the comparison over a 10-day period in February for OBS-1 and OBS-3. The OBS-2 data were intermediate between these two and are not plotted. While a reasonable agreement for the 10-day mean values is achieved (Table 7), measured SSC is seen to be substantially less time-dependent than the simulated values. For example, whereas at OBS-3 the measured mean amplitude of this variation (about the time-mean value) is about 50 mg L^{-1}, the corresponding value for the simulated SSC is about 5 mg L^{-1} in agreement with Fig. 10a. As described next, this order of magnitude difference between simulated and measured amplitudes of SSC requires invocation of a hydraulic open channel analogy of the lake-and-streams system.

LAKE REGIME

Newnans Lake can be viewed as the wide segment of a narrow water course or channel. The up-lake reach of the channel is a notional water course combining Hatchet

Creek and Little Hatchet Creek. Prairie Creek is the down-lake reach of the same channel. Within the lake the speed of the channel current is reduced substantially, while at the same time wind generates waves and a very weak circulation. The combined strength of the current and circulation is only a few millimeters per second.

Suspended sediment is present in the lake at all times, with a representative SSC profile shown in Fig. 15. The SSC gradient, called a secondary lutocline (Ross and Mehta, 1989), defines what may be referred to as a Benthic Suspended Sediment Layer (BSSL) beneath the gradient. The lower level of this weakly non-Newtonian layer is the primary lutocline characterized by hindered settling below this lower lutocline. For the present analysis we may conveniently chose the muck-water surface to represent the lower bound of the BSSL. The BSSL shown does not have a well defined height but it can be taken as 0.80 m based on the "equal area" assumption, which idealizes the water column as composed of a distinct BSSL beneath sediment-free water. This value is a representative mean for the entire period of measurement, with a range of about 0.2 to 1 m.

The thickness of the bottom sediment layer that must be entrained to generate the 0.80 m high BSSL with a mean SSC of about 70 mg L^{-1} (Fig. 15) can be estimated. Taking 100 kg m^{-3} as the dry density of the bed, this thickness is equal to (0.07/100)x0.80 = 0.00056 m = 0.56 mm, which indicates that only a very thin layer of the bed participates in the sediment entrainment process. This finding in turn implies that there is little interaction between the ~ 2 m thick muck in the lake and the water column, because even a BSSL with an unlikely high concentration of, say, 700 kg L^{-1} would correspond to a less than 10 mm thick bed layer.

The persistence of a "constant" BSSL in the lake may be explained on a time-mean basis in terms of the wind kinetic energy required to raise the potential energy of a layer of suspension to the height of the BSSL. Quite simply, wind energy is expended in expanding a 0.56 mm thick bottom layer with a dry density of 100 kg m^{-3} to a 0.80 m high BSSL with SSC of 70 mg L^{-1}. To provide a mechanistic explanation of this phenomenon, Vinzon and Mehta (1998) used the steady state form of the turbulent kinetic energy balance to obtain the equilibrium height H_e of the BSSL as a function of wave properties. The semi-theoretical equation was shown to be

$$H_e = 0.65\left(\frac{(a_b{}^3 k_s)^{3/2}}{T^3 \frac{\rho_s - \rho_w}{\rho_w} g w_o \varphi_v}\right)^{1/4} \tag{8}$$

where ρ_s is the particle density, g is the acceleration due to gravity and $\varphi_v = C/\rho_s$ is the mean volumetric concentration of the suspended solids.

For estimating H_e using Eq. (8) we will choose the following nominal values: a_b = 0.015 m based on Eq. (5b) with H = 0.07 m, T = 1.4 s and h = 1.6 m, k_s = 0.1 m (instead of the secular value of 0.01 m, in order to account for local bottom variability), ρ_s = 1,700 kg m^{-3}, ρ_w = 1,000 kg m^{-3}, w_o = 1.15x10^{-4} m s^{-1}, and φ_v = 70/(1700x1000) = 0.041 x10^{-3}. This yields H_e = 0.68 m, which is within the measured range.

An important basis of Eq. (8) is that it does not embody the concept of a threshold for resuspension (in terms of the bed shear strength τ_s). To account for the presence of suspended sediment in the lake water column at low discharges ($\leq$1 m^3 s^{-1}) and wind speeds ($\leq$2 m s^{-1}), it would be necessary to reduce the shear strength to less than 0.002 Pa, the combined current-wave shear stress under these conditions. Such low shear

strength implies that the sediment in suspension under these conditions consists mostly of organic material with density close to water. At high discharges and wind speeds one can expect heavier particles to be brought into suspension. If so, the composition of sediment leaving Prairie Creek must vary with the hydraulic conditions in the lake, and that, in general, the material would be finer than that at the lake bottom. Qualitative observations of sediment in suspension appear to be consistent with this inference.

To entrain organic matter at very low discharges and wind speeds must require a hydrodynamic forcing mechanism at the bottom. Conceivably it is provided by a relative motion between water and the bottom sediment layer susceptible to movement. Evidence for such likelihood is found in Fig. 16, in which the vertical amplitude of the fluid (muck) acceleration recorded 0.2 m below the muck surface is plotted against wind speed. As the accelerometer data showed numerous discrepancies, only a limited number of data points are included. Despite this limitation, we observe a clear trend of increasing amplitude with wind speed, with 3.2 m s^{-1} as a threshold wind speed marking the onset of muck heave. Heave would suggest a relative motion at the muck surface and associated shear stress that would be absent over a hard bed. In laboratory wave-flume experiments Maa and Mehta (1987) observed interfacial waves at the soft mud surface, and estimated the contribution to bed shear stress from the relative motion between the mud surface and the boundary layer in water. They found that this contribution can be a significant fraction of the bed shear stress estimated from hard bed analysis.

Pore pressure data given in Table 5 corroborate muck movement recorded by the accelerometer. Unfortunately, pore pressure values showed substantial scatter, with little likelihood of obtaining a reliable correlation with wind speed (Jain et al., 2005).

NUTRIENT LOADS

Nutrient data collected at the platform included concentrations of dissolved organic nitrogen, dissolved organic phosphorus, nitrate-nitrite, ammonia, particulate nitrogen, particulate phosphorus, soluble reactive phosphorus, total dissolved nitrogen, total dissolved phosphorus, total Kjeldahl nitrogen and total phosphorus. None of these species, which were obtained during six sets of data collection over the study period, showed any dependence on the wind speed. This was so, in part, because water sampling using the auto-samplers was carried out at 1 to 3 hour intervals over 24 to 72 hr periods. Diurnal variation in nutrient concentrations was apparently too weak to be detected during these periods. At the same time, the sampling duration was insufficiently long for identifying frontal oscillations in concentrations.

Nutrient concentrations were also measured daily by SJRWMD in the streams and the lake (at mid-depth) over different periods: Hatchet Creek and Bee Tree Creek during 2003-2004, Little Hatchet Creek during 1998-2004, Prairie Creek during and 1997-2004 and Newnans Lake in 2004. These synoptic data are evidently important for assessing a nutrient budget for the lake. A plot of the dissolved and total load of total Kjeldahl nitrogen (TKN) against discharge, which is typical of all the species and all the stations, is shown in Fig. 17 for Hatchet Creek. There is little evidence of any significant contribution from the particulate load, presumably because of low SSC in the system as a whole. The same conclusion can be drawn for all the species (Jain et al., 2005). As in Fig. 11, linear data fit implies a constant TKN concentration. Thus, given the discharge time-series for the inflows and outflow and assuming a linear relationship between the load and discharge, it was straightforward to calculate the cumulative mass of TKN over any

desired period, and thereby establish a mass balance for the lake. Similar analysis for carried out for all other species (Jain et al., 2005).

In Table 8, besides TKN we have calculated masses of total phosphorus (TP) and dissolved phosphorus (DP), ammonia (NH_4) and nitrate-nitrite (NOx) for the 10-day "non-event" calibration period in February. The results are given in terms of cumulative inflow mass m_I, cumulative outflow mass m_O (Fig. 18), the difference m_I-m_O and the ratio (m_I-m_O)/m_I. Judging from the last two quantities we conclude that TP and DP were in near balance, but TKN, NH_4 and NOx were exported from the lake. Since an insignificantly thin bottom sediment layer exchanges material with the water column, it appears that over the 10-day period the lake supplied nitrogen from sources not accounted for by the two inflow creeks or the lake bottom. The most likely source is the accumulated nitrogen in the lake water itself, presumably coupled with diffusion from bottom sediment and the effects of bioturbation.

In Table 9 we have presented calculations for the 7-day hurricane period in September. Due to high discharges the cumulative masses are up to two orders of magnitude higher than in February. However, at the end of this event, with the exception of TKN, supply from the inflow creeks exceeded outflow from Prairie Creek. In other words, the lake sequestered incoming nutrients represented *by* m_I-m_O.

CONCLUDING COMMENTS

From the hydraulic point of view, Newnans Lake may be thought of as a shallow and wide open channel in which transport of sediment from the creeks is modulated by wind effects in the lake. Light weight, organic-rich fine sediment particles dominate the

suspended matter, and SSC response to wind occurs over a wide frequency band whose range is determined by the combined forcing due to wind effects and stream discharges.

On a time-mean basis, wind kinetic energy maintains sediment as a Benthic Suspended Sediment Layer with a mean height of about 0.80 m and a mean SSC of about 70 mg L^{-1}. The sediment mass in this suspension is equivalent to less than 1 mm thick bed layer, which suggests that there is little interaction between the ~ 2 m thick muck in the lake and the water column.

Nutrient mass balance analysis is simplified because dissolved nutrient loads are close or nearly equal to total loads, with minor to negligible contributions from the low-concentration particulate matter. Mass balances for phosphorus and nitrogen indicate periods on the order of days over which the lake acts both as a net exporter and a net importer of these nutrients.

ACKNOWLEDGMENT

The authors wish to thank John White (now at the Louisiana State University, Baton Rouge) and Erin Bostic for chemical analyses at the Soil and Water Science Department, and Sidney Schofield and Victor Adams for field installations and data retrieval. Maria Martinez provided critical data and information support from the St. Johns River Water Management District.

REFERENCES

Dean, R. G., and Dalrymple, R. A., 1991. *Water Wave Mechanics for Engineers and Scientists.* World Scientific, Singapore.

Gowland, J. E., Mehta, A. J., Stuck, J. D., John, C. V. and Parchure, T. M., 2005. Organic-rich fine sediments in Florida part II: Resuspension in a lake. *Estuarine and Coastal Fine Sediment Dynamics*, J. P.-Y. Maa, L. P. Sanford and D. H. Schoellhamer eds., Elsevier, Amsterdam, 162-183.

Hamrick, J. M., 1992. A three dimensional environmental fluid dynamics computer code: Theoretical and computational aspects. *Special Report No 317*. Applied Marine Science and Ocean Engineering, Virginia Institute of Marine Science, Gloucester Point, VA.

Hamrick, J. M., 1996. User's manual for environmental fluid dynamics computer code. *Special Report No 331*. Applied Marine Science and Ocean Engineering, Virginia Institute of Marine Science, Gloucester Point, VA.

Hamrick, J. M., 2000. Theoretical and computational aspects of sediment transport in the EFDC model. *Technical Memorandum*, Tetra Tech, Inc., Fairfax, VA.

Jain, M., Mehta, A. J., Hayter, E. J., and McDougal, W. G., 2005. A study of sediment and nutrient loading in Newnans Lake, Florida. *Report UFL/COEL-2005/002*, Coastal and Oceanographic Engineering Program, Department of Civil and Coastal Engineering, University of Florida, Gainesville.

Maa P.-Y. and Mehta A. J., 1987. Mud erosion by waves: a laboratory study. *Continental Shelf Research*, 7(11/12), 1269-1284.

Mehta, A. J., 1991. Understanding fluid mud in a dynamic environment. *Geo-Marine Letters*, 11, 113-118.

Park, K., A. Y. Kuo, J. Shen, and J. M. Hamrick, 2001. A three-dimensional hydrodynamic-eutrophication model (HEM3D): description of water quality and sediment processes submodels. *Special Report* 327, The College of William and Mary, Virginia Institute of Marine Science, Gloucester Point, VA.

Richards, A., 2003. Sea breeze genesis - A missing factor. *MSc thesis*, School of Mathematics Meteorology and Physics, University of Reading, UK.

Ross M. A. and Mehta A. J., 1989. On the mechanics of lutoclines and fluid mud. *Journal of Coastal Research*, SI 5, 51-61.

Soulsby, R., L., Hamm, L., Klopman, G., Myrhaug, D., Simons, R. R., and Thomas, G. P., 1993. Wave-current interaction within and outside the bottom boundary layer. *Coastal Engineering*, 21, 41-69.

Table 1 Instruments deployed at the platform

Property	Instrument make	Model no.	Freq. of bursting (Hz)
Wind	RM Young anemometer	05103	-
Air temperature	Analog Devices gauge	AC 2626	-
Water temperature	Analog Devices gauge	AC 2626	-
Current	Sontek acoustic current meter	Field ADV	10
Air pressure	Trans-metrics gauge	B020	-
Total (H_20) press.	Trans-metrics gauge	P215L	10
Pore (H_20) press.	Druck gauge	PDCR-81	10
TSS	Sea Point sensors (OBS)	-	10
Fluid acceleration	Analog Devices accelerometer	ADXL 202	10
Data logging	Campbell Scientific logger	CR23X	-
Light	Carmanah light	501	-
Data transmission	Airlink Comm. modem	Redwing CDMA	-

Table 2 Coefficients for stress calculation

Coefficient	Value
a_1	-0.06
a_2	1.70
a_3	-0.29
a_4	0.29
M_1	0.67
M_2	-0.29
M_3	0.09
M_4	0.42
N_1	0.75
N_2	-0.27
N_3	0.11
N_4	-0.02
I	0.80

Table 3 Lake physical parameters

Month	Water temperature (^oC)	Rainfall (mm)	Mean wind speed [a] ($m\ s^{-1}$)	Maximum wind speed [b] ($m\ s^{-1}$)	Prairie Cr. discharge ($m^3\ s^{-1}$)
January	16.9	1.3	3.2	10.3	0.64
February	17.5	4.9	4.1	11.4	0.89
March	22.0	1.6	3.7	9.4	1.24
April	24.4	1.0	3.7	12.6	0.92
May	29.3	0.4	3.3	11.1	0.50
June	31.0	5.2	2.6	12.9	0.26
July	32.6	3.2	2.5	8.9	0.21
August	31.9	75.0	3.0	10.5	0.42

[a] Monthly average of ½-hourly (2-min mean) values.
[b] Peak value in a month.

Table 4 Wave parameters at the platform

Month	Maximum wave height [a] (m)	Maximum modal wave period [b] (s)	Max. horz. wave orbital current ampl. (m s^{-1})	Max. vert. wave orbital current ampl. (m s^{-1})	Max. vert. wave orbital acc. ampl. (m s^{-2})
January	0.14	1.2	0.17	0.13	0.45
February	0.14	1.3	0.18	0.13	0.41
March	0.16	1.3	0.20	0.13	1.71
April	0.16	1.4	0.20	0.12	1.58
May	0.14	1.3	0.20	0.15	0.4
June	0.28	1.2	0.47	0.39	0.41
July	0.16	1.2	0.21	0.14	-
August	0.18	1.3	0.23	0.16	2.37

[a] Significant wave height is defined as four times the root-mean-square of surface elevation.
[b] Modal wave period is defined as the period corresponding to the frequency at the wave spectral peak.

Table 5 Current, SSC and pore pressure at the platform

Month	Mean current (mm s^{-1})	SSC-1[a] (mg L^{-1})	SSC-2[b] (mg L^{-1})	SSC-3[c] (mg L^{-1})	Depth-mean SSC (mg L^{-1})	Maximum muck pore pressure (kPa)
January	2.6	7.1	20	176	68	50
February	4.2	8.8	17	155	60	95
March	2.8	12.4	39	254	102	140
April	3.3	12.0	46	239	99	158
May	1.4	9.6	52	230	97	268
June	2.5	8.8	110	119	79	326
July	2.8	6.1	111	116	78	-
August	0.3	3.4	117	-	-	281

[a] OBS-1 elevation 1.8 m above bed; [b] OBS-2 1.4 m; [c] OBS-3 1.1 m.

Table 6 SSC characteristics related to wind speed

Month	OBS elev.[a] (m)	$\overline{C}$			$\hat{C}$		$\hat{C}/\overline{C}$
		$\overline{a}$	$\overline{b}$	@ 4 m s^{-1} (mg L^{-1})	$\hat{a}$	@ 0.5 m s^{-1} (mg L^{-1})	
February	1.8	0.31	7.0	8.2	0.67	0.3	0.04
	1.4	0.25	15.5	16.5	0.77	0.4	0.02
	1.1	0.08	148	162	36.3	18.1	0.11
May	1.8	0.16	8.8	9.4	2.0	1.0	0.11
	1.1	8.2	193	226	10.7	5.4	0.02

[a] With respect to bed surface.

Table 7 Measured and simulated time-mean SSC at the platform

OBS	SSC		Error (%)
	Measured (mg L^{-1})	Simulated (mg L^{-1})	
1	8	7	-13
2	16	20	+25
3	150	113	-25

Table 8 Cumulative nutrient masses during the 10-day non-event period

Species	Inflow (m_I) (t)	Outflow (m_O) (t)	Diff. (m_I-m_O) (t)	(m_I-m_O)/m_I
TP	0.05	0.11	-0.06	-1.2
DP	0.05	0.03	+0.02	+0.4
TKN	0.47	1.76	-1.29	-2.7
NH_4	0.02	0.19	-0.17	-8.5
NOx	0.02	0.09	-0.07	-3.5

Table 9 Cumulative nutrient masses during the 7-day hurricane period

Species	Inflow (m_I) (t)	Outflow (m_O) (t)	Diff. (m_I-m_O) (t)	(m_I-m_O)/m_I
TP	2.6	0.8	-1.8	-0.7
DP	2.6	0.2	-2.4	-0.9
TKN	30.5	13.9	+16.6	+0.5
NH_4	1.19	1.49	-0.3	-0.3
NOx	0.45	0.75	-0.3	-0.7

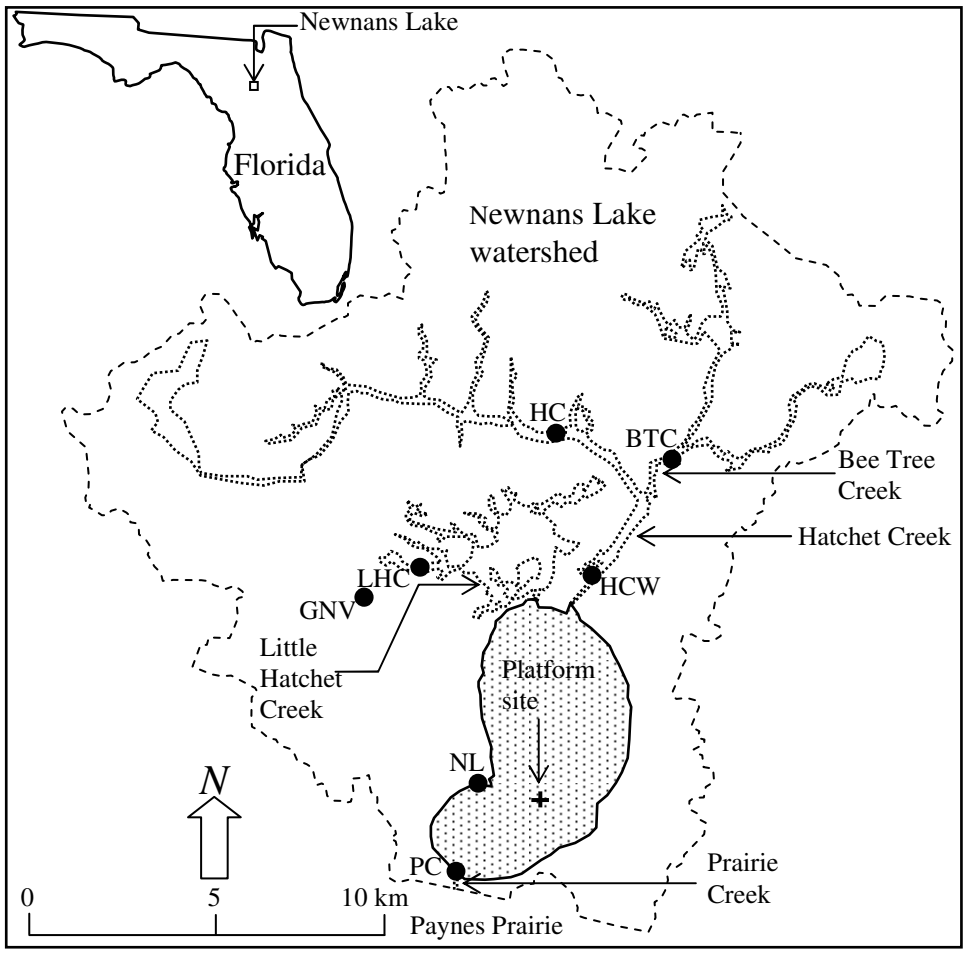

Figure 1 Newnans Lake and watershed in north-central Florida.

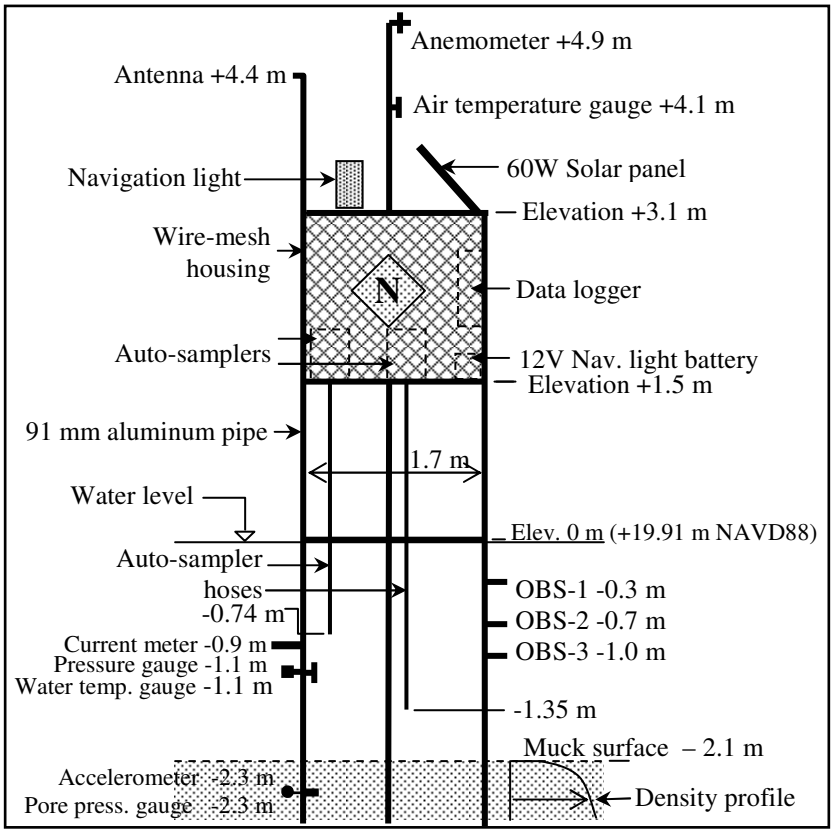

Figure 2 Field platform and instrumentation.

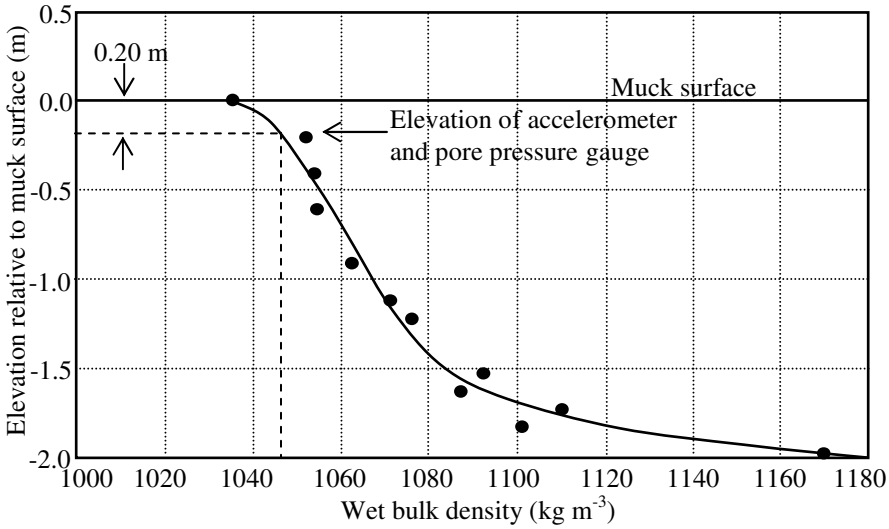

Figure 3 Bottom muck density profile at the platform site.

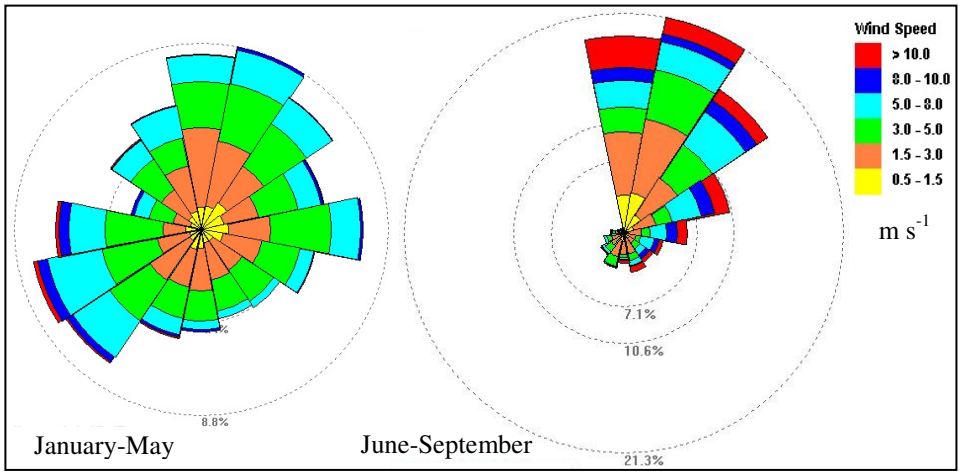

Figure 4 Wind roses for January-May and June-September 2004.

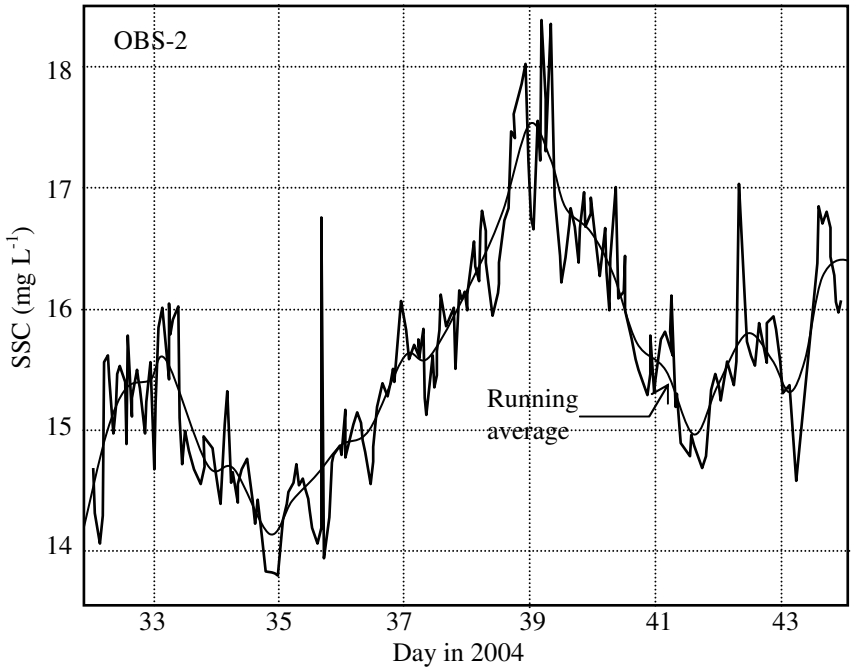

Figure 5 Sample time-series of variation of SSC measured by OBS-2.

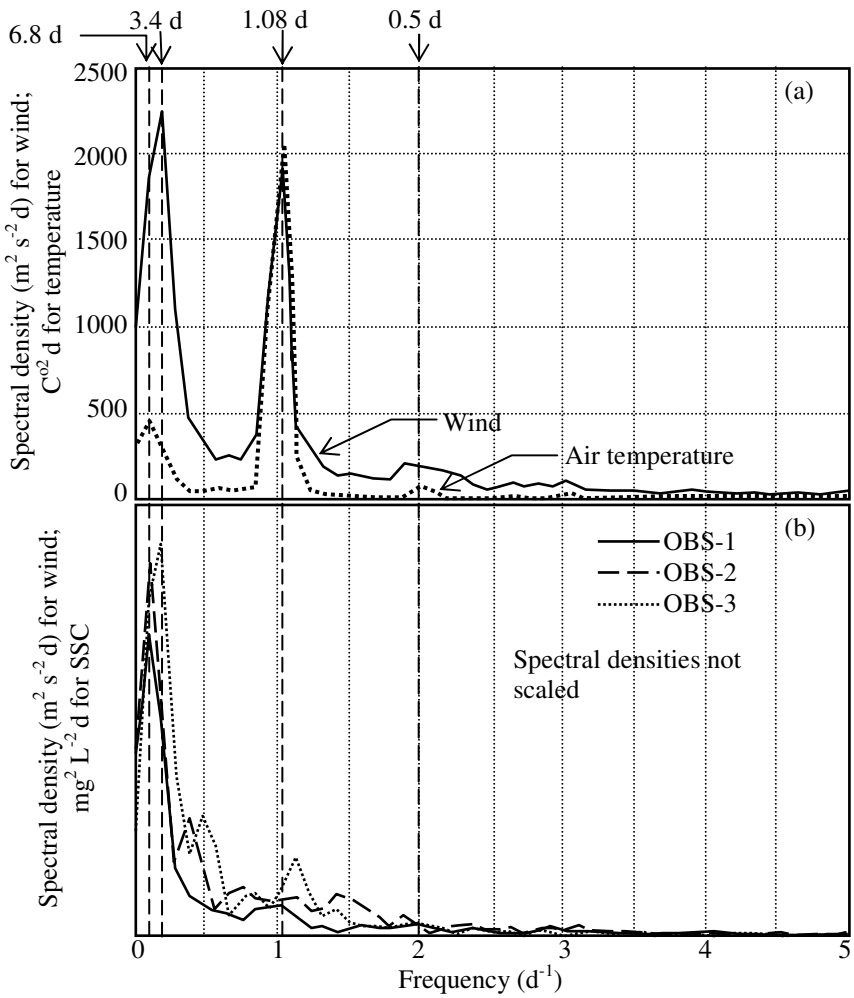

Figure 6 Wind, air temperature and SSC spectra.

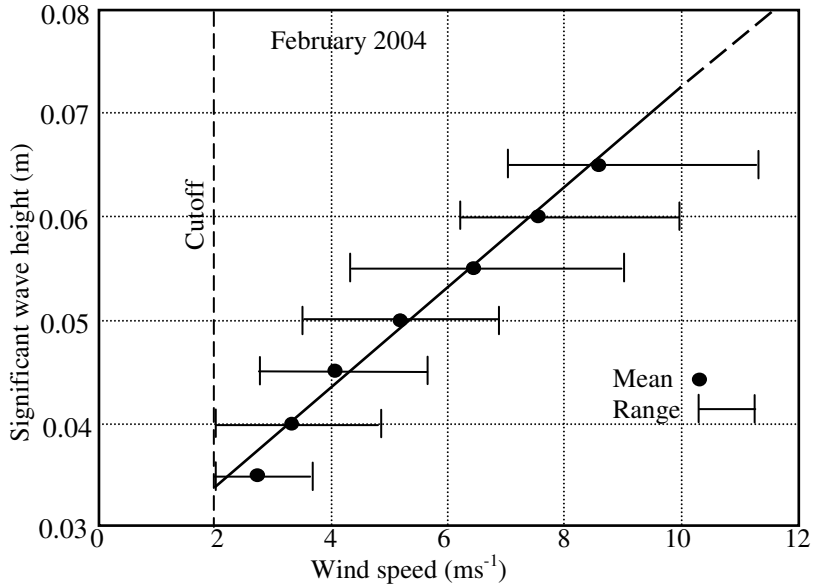

Figure 7 Variation of significant wave height with wind speed.

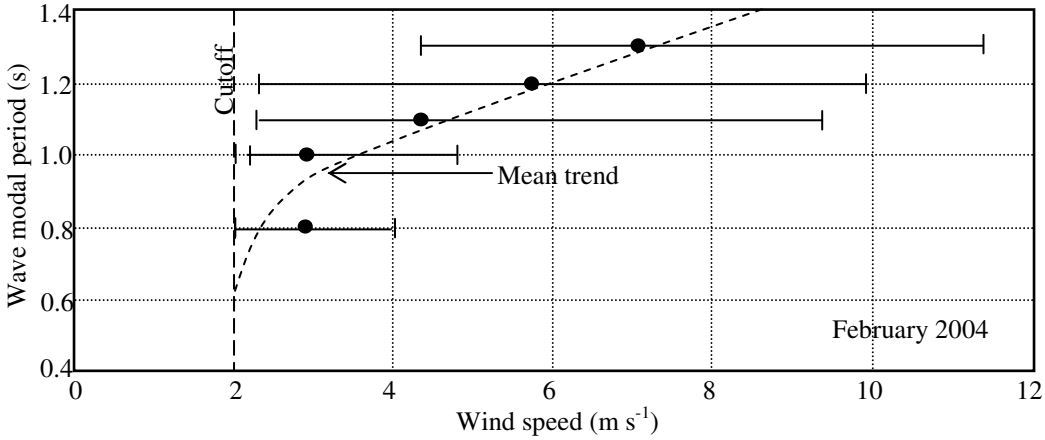

Figure 8 Variation of wave modal period with wind speed.

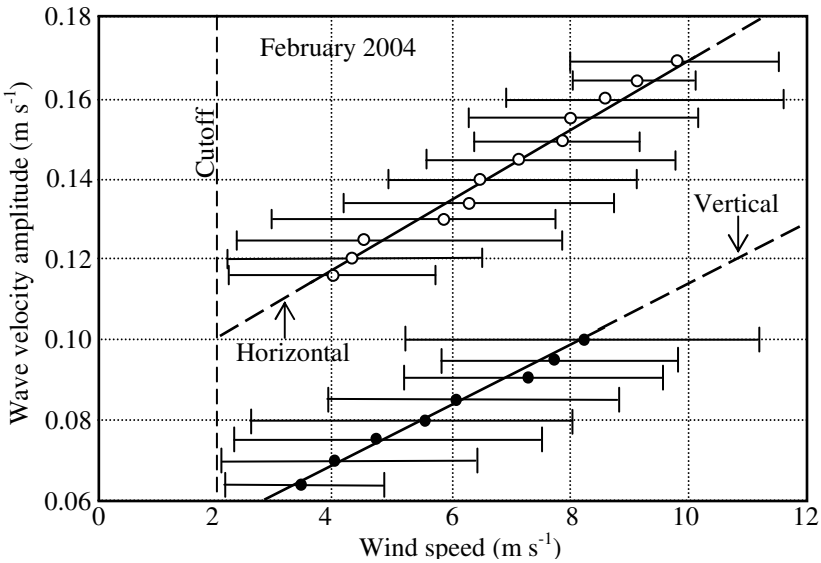

Figure 9 Variation of wave orbital velocity amplitudes with wind speed.

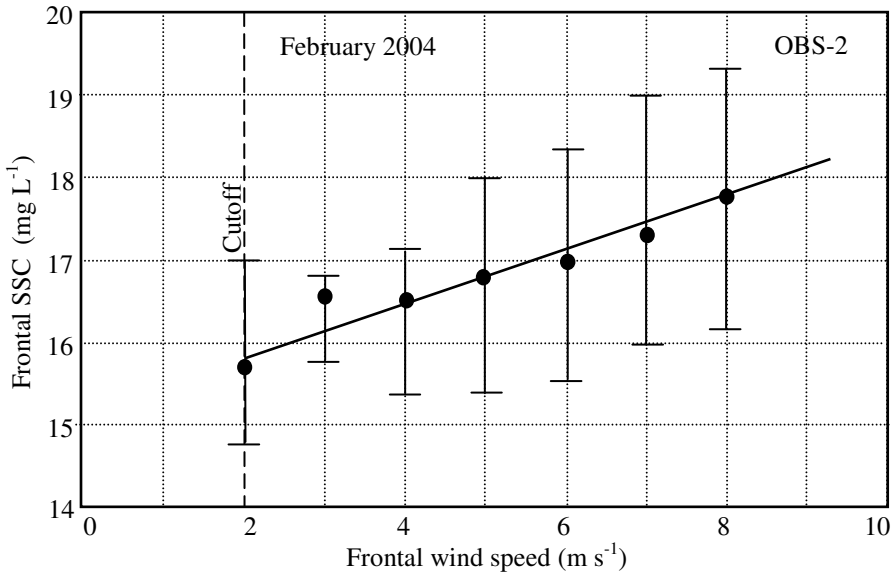

Figure 10a Variation of frontal SSC ($\overline{C}$) with frontal wind speed ($\overline{U}$) at OBS-2.

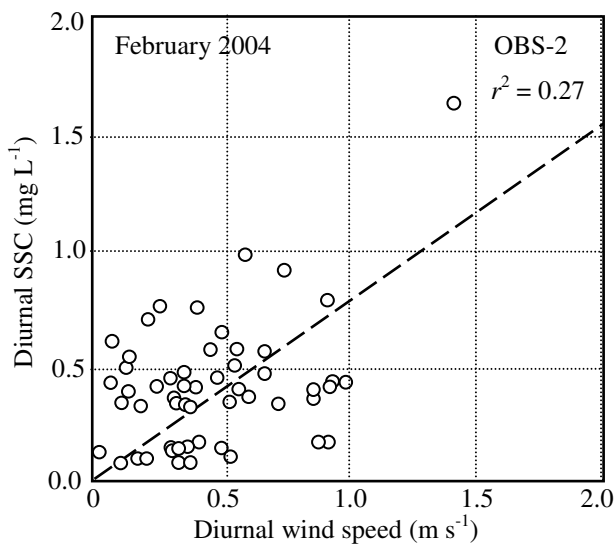

Figure 10b Variation of diurnal SSC ($\hat{C}$) with diurnal wind speed ($\hat{U}$) at OBS-2.

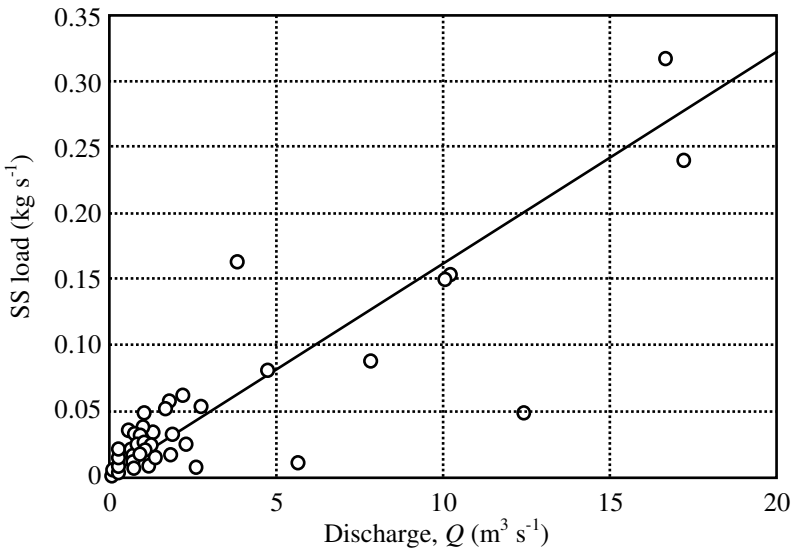

Figure 11 Variation of SSC load with discharge in Prairie Creek.

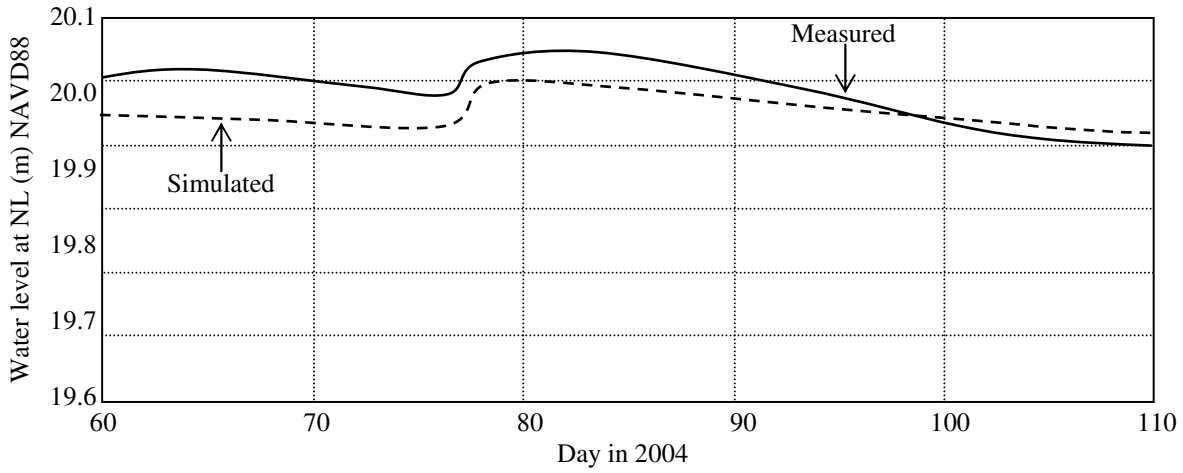

Figure 12 Comparison of measured and simulated water levels in the lake.

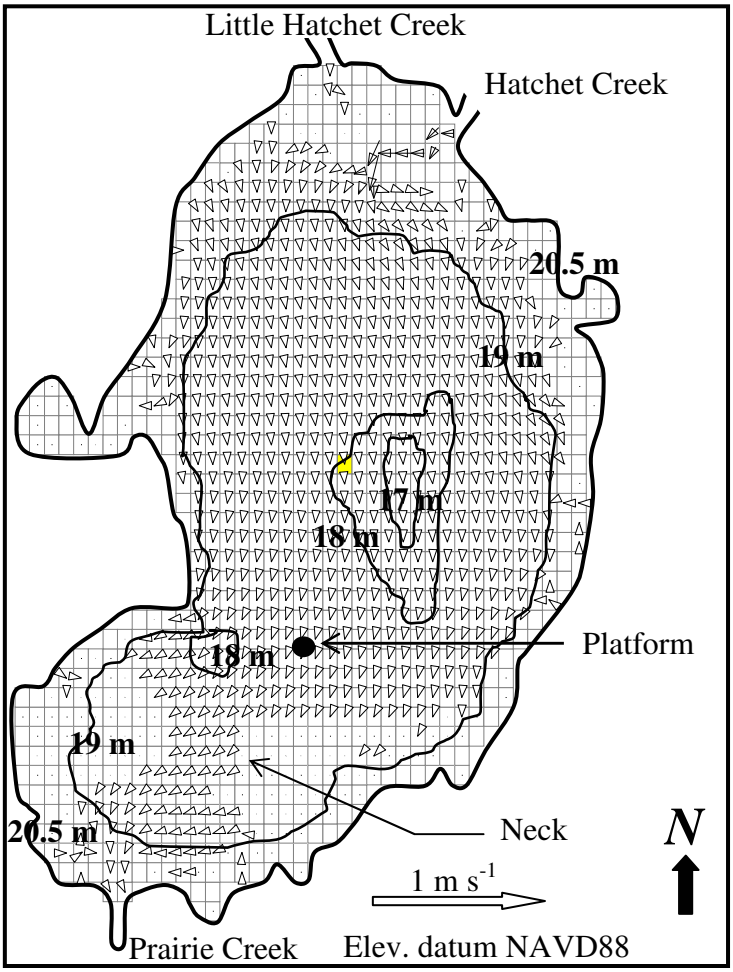

Figure 13 Simulated surface velocity vectors. Selected depth contours are shown.

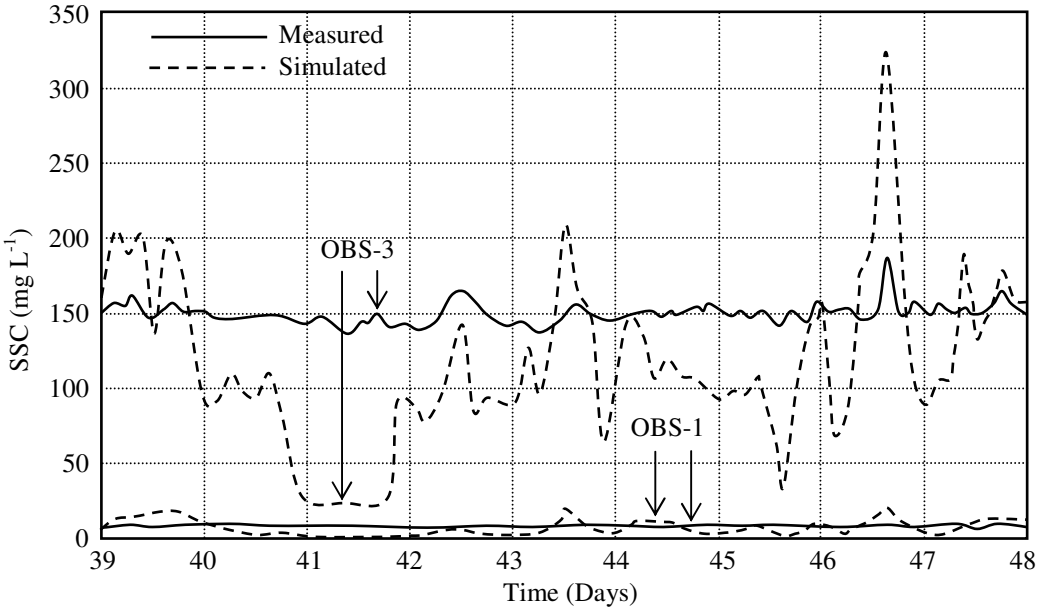

Figure 14 Measured and simulated SSC time-series for OBS-1 and OBS-3.

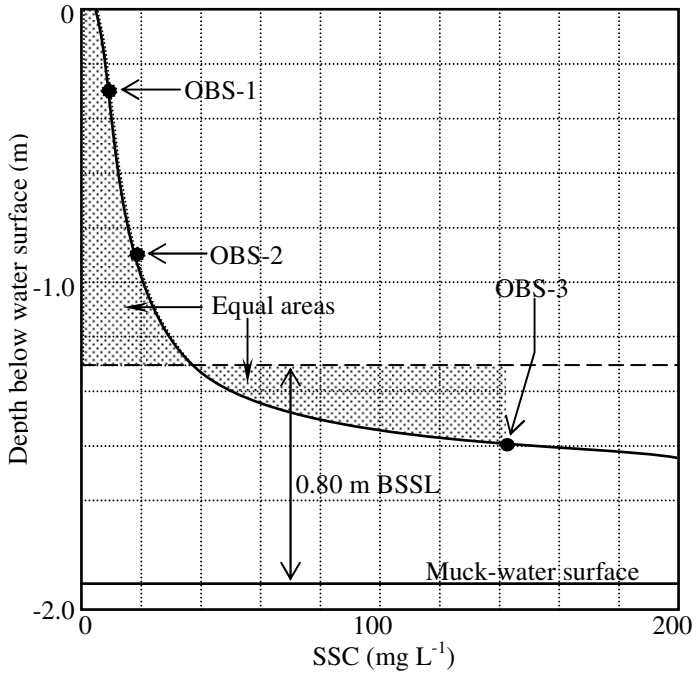

Figure 15 Typical SSC profile and estimation of BSSL height.

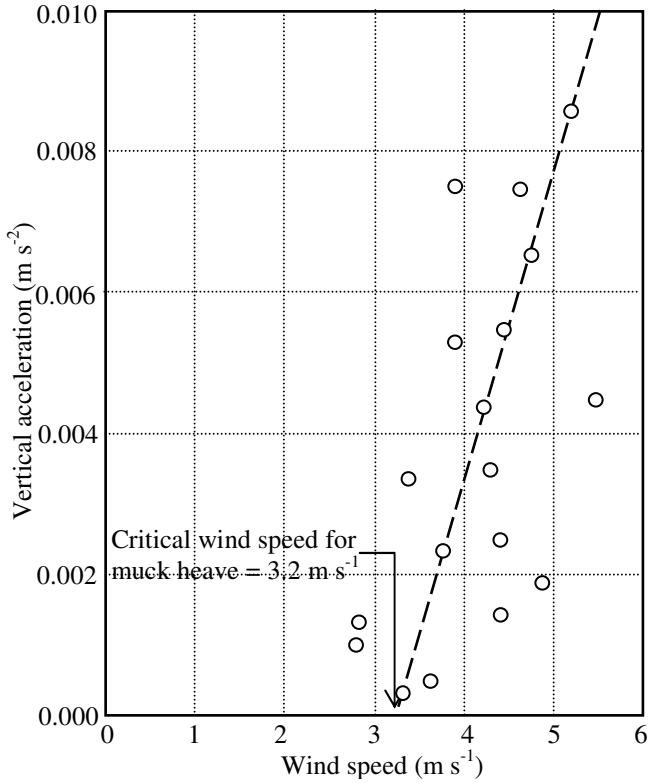

Figure 16 Vertical acceleration in mud versus wind speed during February, March and May.

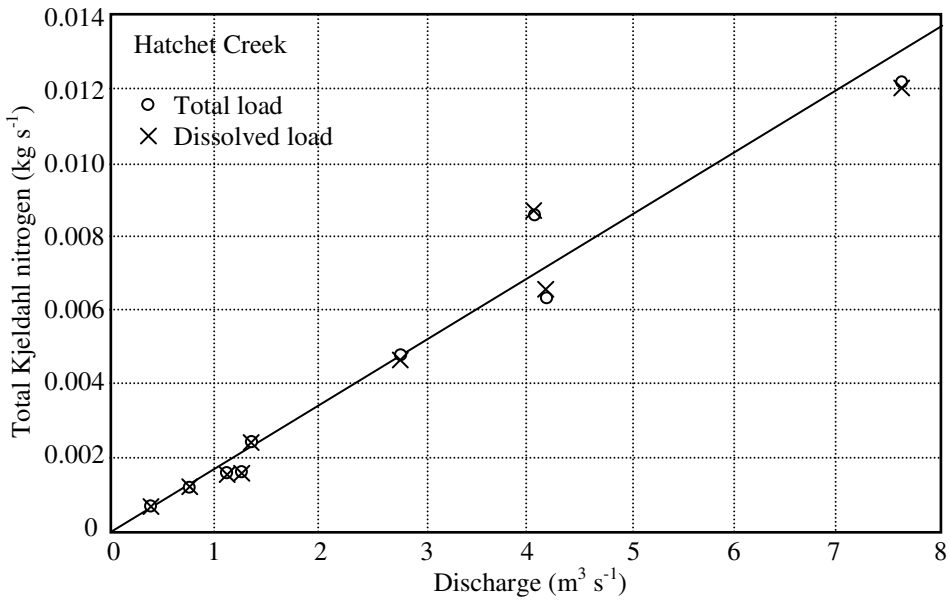

Figure 17 Total load of TKN versus discharge in Hatchet Creek.

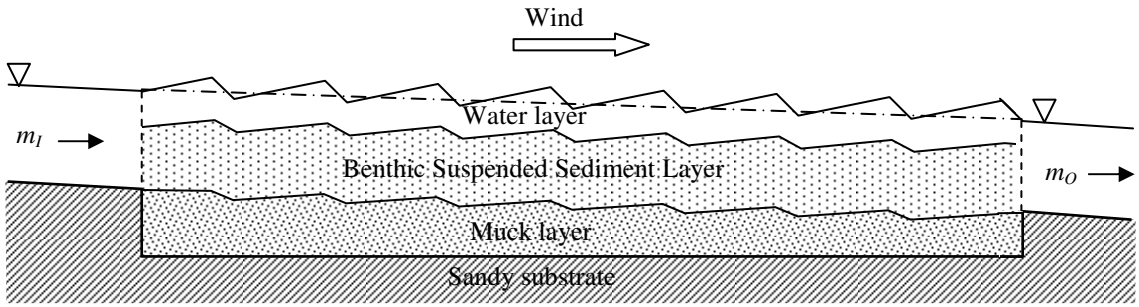

Figure 18 Inflow and outflow nutrient masses.